Eur Biophys J (1987) 14:329–336

European Biophysics Journal

Determination of "active" cytochrome P-450 from relaxation kinetics of product formation

U. Schröder and H. Diehl*

Universität Bremen, Fachbereich 1 – Physik, D-2800 Bremen 33, Federal Republic of Germany

Received March 24, 1986/Accepted in revised form October 1, 1986

Abstract. We estimate the "active" part of cytochrome P-450, which is involved in a special substrate transformation, by measuring the initial change of the production rate as a function of the relaxation transitions between two different steady states of the reaction cycle of cytochrome P-450 using the light-reversibility of the carbon monoxide inhibition. The kinetic data of such relaxations are interpreted within a model cycle, which reduces the reaction cycle to three steps. The estimation of the rate constant of the first reduction step, derived from model simulation of the production rate, is confirmed by independent experimental study of the reduction kinetics.

An application of our model to the O-deethylation of 7-ethoxycoumarin reveals that – in a time average – 10%–15% of the spectroscopically detectable cytochrome P-450 is involved in that transformation.

Key words: Cytochrome P-450, photoreversibility, relaxational enzyme kinetics, 7-ethoxycoumarin

Introduction

Cytochrome P-450 (cyt. P-450), the terminal enzyme of the membrane bound liver microsomal monooxygenation system represents a system of isoenzymes of high multiplicity with respect to the conversion of a variety of substrates (Ullrich 1979; White and Coon 1980). In their membrane bound form the isoenzymes are hardly distinguishable by physical and chemical methods.

One approach to differentiate the multiplicity is based on the isolation of individual isoenzymes of cyt. P-450 for chemical and physical characterization (Guengerich 1983; Ueno et al. 1983; Tsuji et al. 1980; Komori et al. 1984; Ryan et al. 1979, 1984) but no significant correlations have been found between single isoenzymes of cyt. P-450 and their substrate-specifity (Johnson 1979; Bansal et al. 1985). The specific microsomal activity towards different substrates cannot be described by a linear combination of the specific activities of the various forms of cyt. P-450 in reconstituted systems (Guengerich et al. 1982). For that many reasons may exist: (1) the monooxygenation system is partially inactivated by the isolation procedure (Johnson 1979; Bansal et al. 1985), (2) the physico-chemical properties of cyt. P-450, which govern the separation of the isoenzymes, do not parallel its catalytic properties, (3) the different isoenzymes need different membraneous environments for optimal enzymatic activity (Ingelman-Sundberg 1981; Ingelman-Sundberg and Johansson 1980; Imai 1979), (4) there are more isoenzymes not detected so far.

In order to differentiate the multiplicity of substrate-specifity two indirect approaches have been used; measuring the product formed by a single turnover (Andersson et al. 1979) and measuring the initial kinetics in order to obtain the turnover number (Ihlefeld and Diehl 1976; Ruf and Eichinger 1982). However, the low temperature (– 30 °C) used to inhibit the first reduction step (Andersson et al. 1979) may invalidate conclusions concerning the behaviour of the monooxygenase system in its native environment.

The detectable intermediates of the reaction cycle are superpositions of the intermediates of all isoenzymes (Ruf and Eichinger 1982). Only the kinetics of specific product release will be valuable in differentiating the multiplicity of substrate specificity. In particular, the pre-steady state kinetics of

* To whom offprint requests should be sent

Abbreviations: Cyt. P-450 = microsomal cytochrome P-450, 7-EC = 7-ethoxycoumarin

product formation have to be evaluated. For that purpose we partly inhibit the monooxygenase activity by applying different $CO:O_2$ mixtures to the enzymatic assay. We use the photoreversibility of the CO-dependent inhibition to induce relaxation-transitions between two steady-states of the reaction cycle (Ihlefeld and Diehl 1976).

A kinetic model of the reaction cycle is introduced. It enables us to determine the turnover number of the model for a special transformation.

The model is able to predict effects on the enzymatic transformation rate, which result from definite changes of external parameters in the reaction assay, e.g. the partition of carbon monoxide and oxygen or the photodissociating light intensity.

From the turnover number, determined from the initial product formation kinetics, the partition coefficient of the total cyt. P-450 in the 7-ethoxycoumarin-deethylation is estimated.

Materials and methods

Materials

Fresh pig livers were obtained from the communal slaughterhouse. The preparation of the pig liver microsomes (Lu and Levin 1971), the determination of protein content (Peterson 1977) and cyt. P-450 content (Omura and Sato 1964) were carried out by standard procedures.

7-ethoxycoumarin (7-EC), NADPH, catalase and glucose oxidase were purchased from Boehringer Mannheim, FRG; 7-hydroxycoumarin and D-glucose from Merck, Darmstadt, FRG. All chemicals were of the highest available grade.

Flash-photolysis method

The standard assay for the flash-photolysis experiments contained pig liver microsomes (about 0.6 mg/ml of microsomal protein), 0.2 mmol/l NADPH, 5 mmol/l $MgCl_2$, 0.1 mmol/l 7-EC and 50 mmol/l *Tris*/HCl buffer, pH 8.0, in a total volume of 0.5 ml in a quartz cuvette of 5 mm optical path length. The temperature was held at (25.0 ± 0.1) °C.

In the photoreversibility experiments we irradiated the sample with monochromatic light of high intensity (max. 40 mW/cm^2) at the absorption wavelength of the ferrous cyt. P-450 (Fe^{2+})-CO complex (450 nm, bandwidth 20 nm). The irradiation time τ (20 ms – 100 s), the time of darkness between two flashes δ (> 20 ms), the number of flashes n, which constitute one irradiation sequence, and the irradiation power are variables (Fig. 1 a).

The apparatus and the techniques of measurement have been described elsewhere (Ihlefeld and Diehl 1976). We measured product formation increases, $\Delta P(\tau, n, \delta)$, by monitoring the fluorescence increase of 7-hydroxycoumarin using a modified MPF-3 fluorescence spectrophotometer (Perkin-Elmer) (Ullrich and Weber 1972). 7-hydroxycoumarin is the main product of the monooxygenation of 7-EC (Jung et al. 1985). ΔP is obtained as the separation between the extrapolated fluorescence intensity versus time plots that develops during the illumination sequence (Fig. 1 b). In order to improve the signal to noise ratio we measure a relative product formation increase, $\Delta P_{rel}(\tau, n, \delta) := \Delta P(\tau, n, \delta)/n\Delta P(\tau_0, n_0 = 1)$ using the $\Delta P(\tau_0)$ of the first flash in each experiment as an internal standard. In addition, this enables us to test the stability of the enzymatic assay.

Stopped flow method

A reaction mixture containing 100 nmol/ml of 7-EC (if substrate is required) and 0.1 mmol/ml *Tris*/HCl buffer, pH 8.0, is loaded into two syringes. In addition, one syringe contains microsomes (3 mg protein/ml) while the other one contains NADPH (1 µmol/ml). Both solutions are gassed with CO ($O_2 < 0.3\%$) for 10 min. The remaining dioxygen is removed by a system of glucose (60 µmol/ml), glucose oxidase (0.1 mg/ml) and catalase (3,000 units/ml) as described

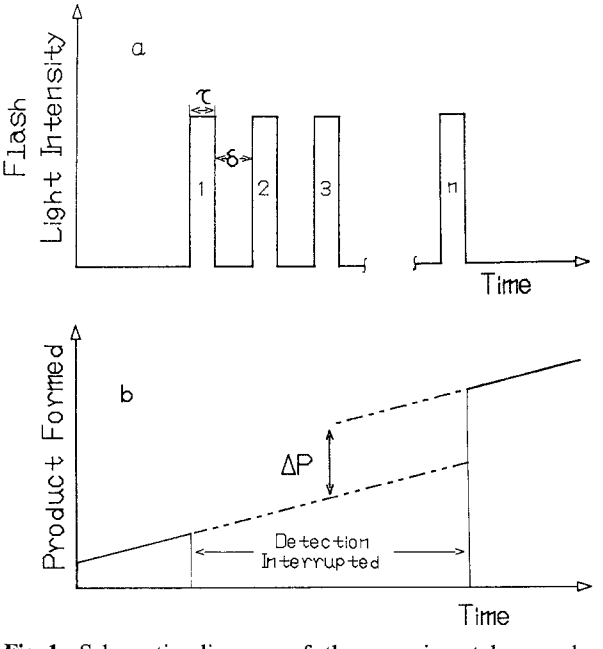

Fig. 1. Schematic diagram of the experimental procedure. During a sequence of illuminations (**a**) the product measurement is interrupted (**b**). τ = period of irradiation; δ = period of darkness; n = number of flashes

elsewhere (Peterson et al. 1976). Prior to the loading of the reaction mixtures into the drive syringes of the AMINCO-Morrow Stopped-Flow Apparatus the drive syringes were gassed with N_2 ($O_2 < 0.1\%$) and filled with a buffer solution containing the above mentioned O_2 scavenging system. The buffer solutions were allowed to equilibrate for 0.5 h, a time long enough to deoxygenate the drive syringes (Gibson et al. 1964). The anaerobic reduction is started by rapid mixing of equal volumes of NADPH and microsomes at a temperature of 25 °C.

The absorbance change between 450 nm and 490 nm is monitored with an AMINCO DW 2 Spectrophotometer connected to a Transient Recorder (DD 1100, Siemens). It enables us to use three linear time scales with a high initial resolution on a long reaction time scale (Ruf 1980). The error of the kinetic data is of the order of ± 3% of the total absorbance change when averaging three runs.

Modeling

The model cycle. The model cycle simplifies the hypothetical reaction cycle (White and Coon 1980) of cyt. P-450 to two irreversible, rate limiting steps (r_1, r_2) and a competitive association and dissociation of carbon monoxide (k_1^+, k_1^-) and dioxygen (k_2^+, k_2^-) (Fig. 2). The photo-dissociation of the cyt. P-450 (Fe^{2+})-CO complex is described by an additional rate constant k^*, which is proportional to the irradiation intensity.

Assuming that the reaction kinetics are governed by pseudo first-order reactions we deduce a linear differential equation system from the model cycle. For real eigenvalues this equation system is solved by a sum of 3 exponential functions (phases) with real exponents, which describes the relaxation of each intermediate of the model cycle towards both its steady states, the dark state, and the illuminated state. To a first approximation the fast phase of the system relaxation is caused by the relaxation of the 5-coordinated Fe^{2+} intermediate (x_2) towards its equilibrium with both 6-coordinated Fe^{2+} intermediates (x_1, x_3). Since x_2 is in rapid equilibrium with its neighbours (x_1, x_3) the amplitude of the fast phase is negligible in the time course of the product forming intermediate $x_3(t)$, which is therefore approximated by a sum of two independent exponential functions. We obtain almost the same time course for $x_3(t)$ when setting $dx_2/dt = 0$ in the differential equation system. This approximation holds as long as the association of CO and O_2 with the cyt. P-450 are fast enough to suppress the concentration of the five-coordinated cyt. P-450 (Fe^{2+}) intermediate (x_2).

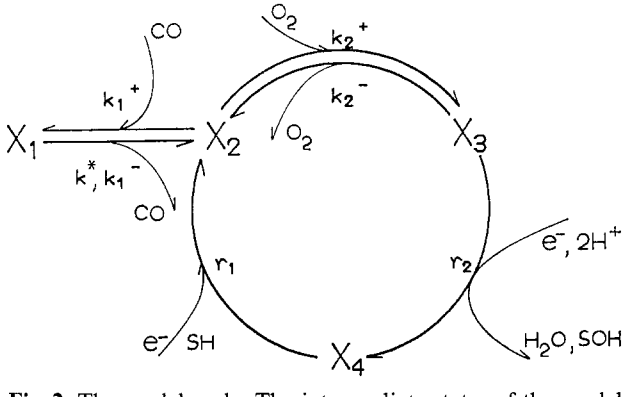

Fig. 2. The model cycle. The intermediate states of the model cycle, x_i, are defined as follows: x_1 = SH-Fe^{2+}-CO, x_2 = SH-Fe^{2+}, x_3 = SH-Fe^{2+}-O_2, x_4 = Fe^{3+}. Fe^{2+} and Fe^{3+} characterize the cyt. P-450 in its different valence states. SH = substrate, SOH = product, e^- = reduction equivalent. k_i, r_i are explained in the text

We define a normalized product formation increase $\Delta P(\tau, n, \delta)$ (Fig. 1 b) caused by one irradiation sequence (1)

$$\Delta P(\tau, n, \delta) = r_2 \left[\sum_{i=1}^{n} \int_0^{\tau} \Delta x_{3i}^L \, dt + \sum_{i=1}^{n-1} \int_0^{\delta} \Delta x_{3i}^D \, dt + \int_0^{\infty} \Delta x_n^D \, dt \right]$$

with

$$\Delta x_{3i}^L = x_{3i}^L(t) - x_{3\infty}^D, \quad \Delta x_{3i}^D = x_{3i}^D(t) - x_{3\infty}^D \tag{2}$$

$r_2 x_3^D(t)$ and $r_2 x_3^L(t)$ describe the production rates in the darkness and under irradiation, respectively, $r_2 x_{3\infty}^D$ the steady state production rate in the darkness.

In the case where $n = 1$, Eq. (1) simplifies to

$$\Delta P(\tau) = r_2 \left[\int_0^{\tau} \Delta x_{3,1}^L \, dt + \int_0^{\infty} \Delta x_{3,1}^D \, dt \right]. \tag{3}$$

The relaxation of the product formation increase $\Delta P(\tau)$ towards its steady state is therefore described by the same number of phases as the relaxation of $x_3(t)$.

Fit procedure. Assuming a superposition of independent first-order reactions, the kinetic data obtained with both methods are analysed by DISCRETE, a nonlinear least square fit-program (Provencher 1976). It describes the time course of the data as a sum of exponential functions:

$$a(t) = a_\infty + \sum a_i \exp(-\lambda_i t).$$

The program is completely automatic in that the only input is the data; no potentially biased initial estimates of either the number or values of the amplitudes a_i and the rate constants λ_i are needed.

The constants of the model cycle are obtained by solving the equations for the relaxation parameters a_i, λ_i. Boundary conditions of the fit procedure are the steady state parameters describing the CO inhibition, the light sensivity and the dioxygen concentration sensitivity of the deethylation reaction under consideration.

Results

1. *Flash-photolysis method*

Product formation by single flash irradiation ($n = 1$). Single flash irradiation results (irradiation time $0.05\,s \leqq \tau \leqq 40\,s$) are presented (Fig. 3) as plots of the relative amount of product formed, $\Delta P_{rel}(\tau)$, against irradiation time (τ). $\Delta P_{rel}(\tau)$, defined as $\Delta P_{rel}(\tau) = \Delta P(\tau)/\Delta P(\tau = 20\,s)$, rises steeply for short values of τ, at longer irradiation times $\Delta P_{rel}(\tau)$ is linearly dependent upon τ (Fig. 3, insert). This indicates the relaxation of the reaction cycle to a new steady state during the irradiation time; this relaxation appears to be complete within 5 s. The best fit to the relaxation data is the sum of two exponential functions (phases). A semilogarithmic plot of the data from Fig. 4 demonstrates the biphasic relaxation of ΔP_{rel}. With all preparations tested and under all conditions of measurement two phases are necessary to fit the data, when 7-EC was used as the substrate. Whenever a third phase was found, it was rejected by means of a Fisher test (Provencher 1976).

Model tests. The relaxation parameters depend on the conditions under which the measurements are carried out. We use that dependence to test the proposed model. Figure 3 shows values of ΔP_{rel} (single flash irradiation) for two different CO/O_2-ratios. At the high CO/O_2 ratio both the rate of increase of ΔP_{rel} and the amount of product formed in the pre-steady state are reduced. The solid line in Fig. 3 represents the best fit to the data obtained at the high CO/O_2-ratio; the parameters from this fit were then used in a computer simulation to produce the fit for the data obtained at the low CO/O_2 ratio (Fig. 3, dashed line). Only the value of k_1^+ needed to be changed to get this fit.

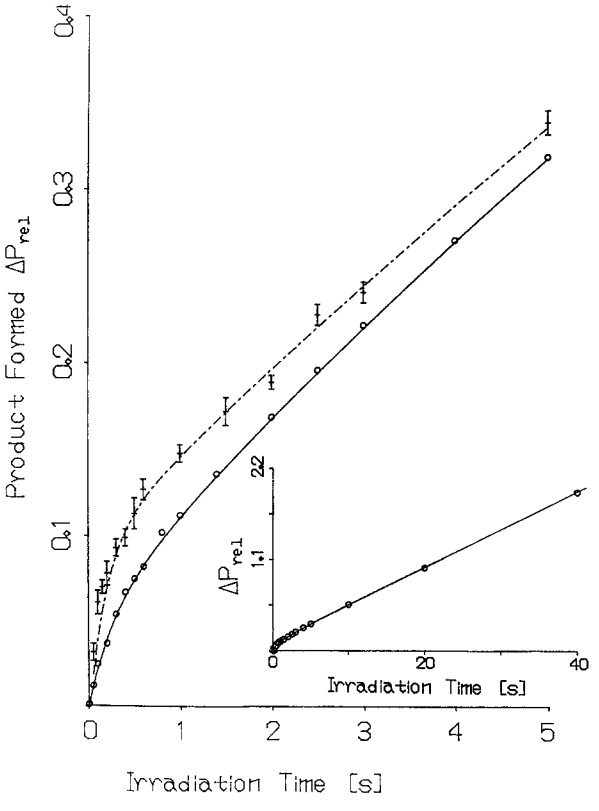

Fig. 3. Relative product formation increase, $\Delta P_{rel}(\tau)$, for two different CO contents. The assay is gassed with a mixture of $N_2:CO:O_2$ with the following ratios: (*a*) 40:50:10, —— best fit of the data ○ (curve is part of the insert), (*b*) 80:10:10, + data, –·– calculated from the result of the best fit of the data ○ from (*a*). Enzymatic assay, see materials and methods

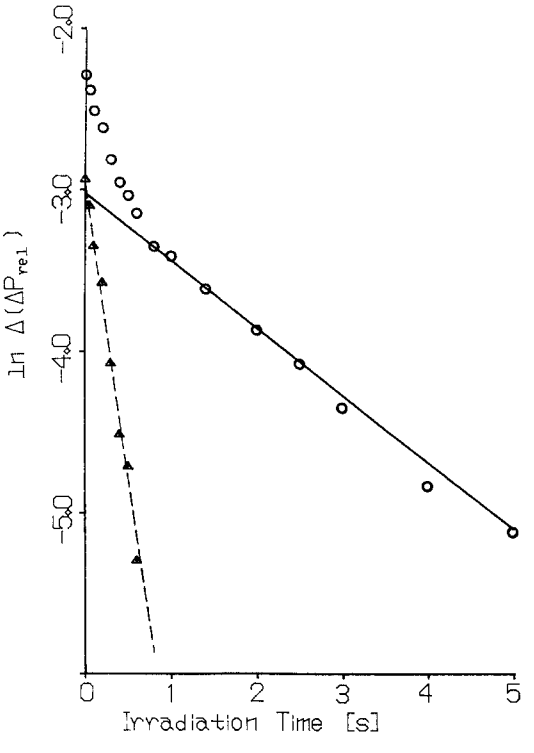

Fig. 4. Relaxation of the relative product formation increase into the steady state. $\Delta(\Delta P_{rel}(\tau)) = \Delta P_{rel,\infty}(\tau) - \Delta P_{rel}(\tau)$. $\Delta P_{rel,\infty}(\tau)$ is the product formation increase extrapolated from the linear part of the curve as shown in Fig. 5. —○—, $\ln\Delta(\Delta P_{rel}(\tau))$; – –△– –, separated fast phase of the relaxation. Data taken from curve (*a*) in Fig. 3

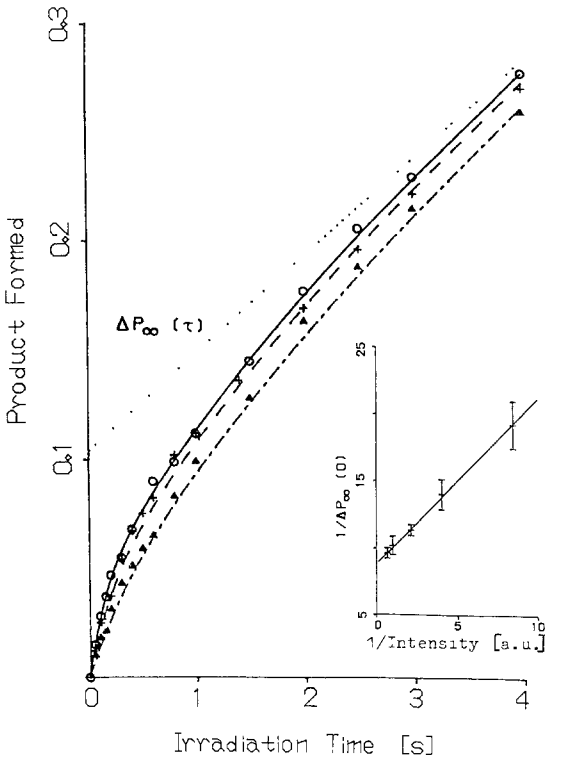

Fig. 5. Relative product formation increase for three different irradiation intensities. ○, intensity $I = I_0 = 38\ \mathrm{mW/cm^2}$; ——, best fit of the data; +, $I = 0.68\, I_0$; – – –, calculated from the result of the best fit of the data (○); ▲, $I = 0.32\, I_0$; –·–·–, calculated as above. The insert shows the double reciprocal plot of the ordinate intercept $\Delta P_\infty(0)$ extrapolated from the linear part of the product formation versus time plot. The irradiation intensity I is changed as indicated. Conditions as in Fig. 3a

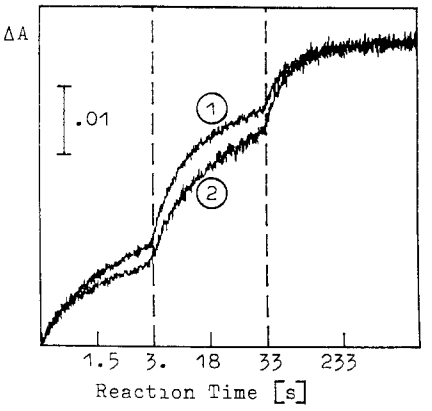

Fig. 6. Anaerobic reduction kinetics. Partial pressure of CO: *1* atmosphere. The absorbance change ΔA (450–490 nm) is plotted versus reaction time. *1*, microsomes with $10^{-4}\,M$ 7-EC; *2*, microsomes without 7-EC. Enzymatic assay, s. materials and methods

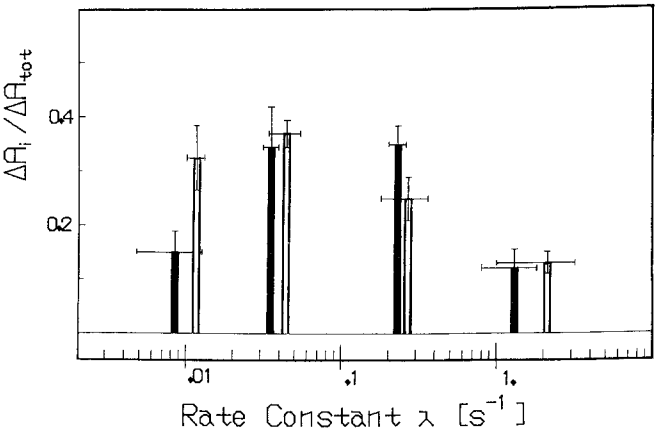

Fig. 7. Results of DISCRETE-fits for the anaerobic reduction kinetics. The amplitudes of the relative absorbance changes $\Delta A_i/\Delta A_{tot}$ referring to the different exponential phases i are plotted versus the rate constant λ of these phases. *Open bars*, microsomes without 7-EC; *solid bars*, microsomes with $10^{-4}\,M$ 7-EC

A second variable in the conditions of measurement is the irradiation intensity. A decrease in the intensity decreases both the amplitude and the rate of the fast phase of product formation (Fig. 5). The solid line in Fig. 5 is the best fit to the data obtained with the highest irradiation intensity. The dashed lines are simulations using the parameters obtained from this fit.

$\Delta P_\infty(0)$ (Fig. 5), which is defined as the ordinate intercept extrapolated from the linear part of the relaxation curve (Fig. 3, insert) serves as an indicator of the contribution of the pre-steady state to the product formed by one irradiation. Because $\Delta P_\infty(0)$ can be measured for a wide range of irradiation intensities we have investigated the intensity dependence of this parameter. Using the approximation $dx_2/dt = 0$, the model predicts a linear relationship between the inverse intercept, $\Delta P_\infty(0)^{-1}$, and the reciprocal intensity (Fig. 5, insert). The intercepts calculated from the data of the relaxation at the highest irradiation intensity are in good agreement with the measured $\Delta P_\infty(0)$.

2. *Stopped-flow method*

A rapid mixing experiment was carried out in order to compare the model parameter r_1, obtained from the fit to the ΔP_{rel} variation, with the first reduction step in the reaction cycle of the cyt. P-450. This first reduction step – the reduction of the ferric cyt. P-450 – is measured anaerobically under an atmosphere of CO by monitoring the corresponding absorbance change, $\Delta A(t)$. Figure 6 shows typical absorbance changes. Addition of 7-EC accelerates the initial reduction velocity but does not influence the extent of the reduction.

Analysis of the reduction kinetics using DISCRETE shows that 4 independent (exponential)

phases are required for an accurate fit. The number of phases does not depend on the presence of the substrate. These results are confirmed by the findings of Ruf (1980) and Ferreira da Silva and Diehl (1985).

Figure 7 shows the results of the best fits. 7-EC does not significantly change the rate constants of the reduction phases, but it does increase the amplitude of the second phase and decrease the amplitude of the fourth phase.

Discussion

Monitoring pre-steady state kinetics of intermediates (Ruf and Eichinger 1982) may be useful in detecting the "active" part of the spectroscopically detectable cyt. P-450 in the microsomal membrane, if the substrate has a significant influence on these kinetics. For substrates like 7-EC, which has a very small effect on the reduction kinetics (Fig. 6), this method is not practical. Therefore, we employ the method introduced by Ihlefeld and Diehl (1976) and establish a model cycle, which enables us to calculate rate limiting steps from product formation. The disadvantage in calculating the rate parameters of a whole reaction cycle only from the time distribution function of one intermediate can be overcome, if the pre-steady state kinetics of the "active" cyt. P-450 become detectable.

The proposed model cycle (Fig. 2) is in accord with the widely accepted assumption of two rate limiting steps in the reaction cycle of the cyt. P-450 – the first and second reduction steps (Werringloer and Kawano 1980; Werringloer et al. 1982; Ruf and Eichinger 1982; Guengerich 1983). This is supported by the biphasic relaxation of $\Delta P_{rel}(\tau, n=1)$ (Fig. 4). The assumption of pseudo first-order reactions is based on the observation of rapid reduction of the electron transferring enzymes by NADPH compared with the two reduction steps of the cyt. P-450. In preliminary studies of the steady state reduction level of cyt. b_5 during NADPH supported aerobic O-deethylation, we find only a very small reoxidation of the cyt. b_5 as compared with the reduction level, when only NADH is applied to the sample (b_5^{red} (NADPH)/b_5^{red} (NADH) > 0.95). This is supported by the increasing b_5^{red} steady state level with increasing pH, which is correlated with a decreasing additional reduction of the cyt. b_5, when NADH is added to the NADPH containing reaction assay (Werringloer et al. 1982).

To test the applicability of the proposed model we change the CO content and irradiation intensity. Their effects on relative product formation are indeed well simulated by the model (Figs. 3–6).

The data provided by the steady state measurements indicate an identical sensitivity of the product forming cyt. P-450 to CO-inhibition and its light reversibility (unpublished results). This supports the assumption of only one kinetic reaction cycle instead of a superposition of two kinetically different cycles. But considering the various forms of cyt. P-450 and their different substrate affinities a superposition cannot be precluded. We tried to test this assumption by calculating $\Delta P_{rel}(\tau)$ and $\Delta P_{rel}(\tau_0, n_0, \delta) := \Delta P(\tau_0, n_0, \delta)/n_0 \Delta P_{rel}(\tau_0)$ as a function of τ and δ.

With the assumption of a superposition of two independent reaction cycles, that differ only in r_1 for the slower phases of the anaerobic reduction (Fig. 7), no additional phase will become detectable, if we simulate $\Delta P(\tau)$ within experimental error. However, calculating $\Delta P_{rel}(\tau_0, n_0, \delta)$ as a function of the period of darkness (δ) in principle a third, slow phase should become detectable, as in the case under consideration the first reduction step dominates the slow phase of $\Delta P_{rel}(\tau_0, n_0, \delta)$. Indeed the measured $\Delta P_{rel}(\tau_0, n_0, \delta)$ reaches a value of only ~ 0.95 at 15 s (data not shown), and on extending the period of darkness we find no further increase. Therefore we interpret the fact that the asymptote is < 1 is a consequence of the inhomogeneous irradiation intensity, which is caused by light scattering in the sample and followed by diffusion of the fluorescent product. The time dependence of $\Delta P_{rel}(\tau_0, n, \delta)$ indicates that a system with reduction rates comparable with the rates of the two slow phases of the anaerobic reduction (Fig. 7) does not contribute significantly to the 0-deethylation of 7-EC.

On the other hand, isoenzymes with slightly different turnover numbers cannot be discriminated by this method as well as the contribution of isoenzymes with higher reduction rates. Thus, the calculated r_1 (Table 1) represents a weighted mean of the reduc-

Table 1. Rate limiting steps (r_1, r_2) and turnover number (tn) of the model cycle. Calculation from the data obtained from single flash photolysis under the conditions indicated. CO/O_2 represents the partial pressure ratio, I_{rel} a relative intensity with I_{rel} (25 mW/cm²) = 1. Only one preparation is used. Enzymatic assay, see materials and methods. Errors represent SD

Conditions		Rate constants		
CO/O_2	I_{rel}	r_1 [s^{-1}]	r_2 [s^{-1}]	tn [min^{-1}]
5	1	0.23 ± 0.03	–	–
	1	0.30 ± 0.12	0.45 ± 0.17	10.8 ± 3.1
	1.5	0.26 ± 0.04	0.47 ± 0.08	10.0 ± 1.2
	0.47	0.34 ± 0.18	0.63 ± 0.22	13.2 ± 4.8
1	1	0.39 ± 0.12	0.65 ± 0.32	14.6 ± 3.9
weighted mean		0.25 ± 0.04	0.49 ± 0.07	10.6 ± 1.5

tion rates of the isoenzymes involved. Since – at 0.1 mM 7-EC – the isoenzymes with high affinity towards 7-EC ($K_M = 1.8\,\mu M$) contribute about 70% to the total activity, these forms essentially determine the relaxation of product formation. Therefore the calculated r_i are estimates for the rate limiting velocity constants of these forms. However, a participation of at least two different high-affinity-forms for 7-EC in liver microsomes of untreated pigs cannot be excluded (H. Graf 1986, personal communication).

The relaxation kinetic data are not sufficient to determine the complete set of the model parameters. Using the data of both the relaxation of the product increase and steady state experiments we determine the complete set of the model parameters by measuring the production rate only. Therefore, interference in the data by "inactive" cyt. P-450 can be neglected.

The two rate limiting steps of the model cycle are insensitive to variations in the CO content and the irradiation intensity (Table 1).

The rate constant $r_1 = (0.25 \pm 0.04)\ s^{-1}$ indirectly calculated from the product formation approaches the rate constant of the second phase of the anaerobic reduction of the cyt. P-450, $\lambda_2 = (0.23 \pm 0.03)\ s^{-1}$. As we interpret the multiple phases of the reduction kinetics to be a consequence of multiple forms of isoenzymes which obey different reduction kinetics, the accordance between the model rate constant r_1 and the measured rate constant λ_2 supports the validity of the proposed model: the rate constant of the step, which is considered to be the first reduction step in the catalytic cycle, agrees well with the rate constant of that reduction phase the amplitude of which is increased by 7-EC.

The "active" part of the cyt. P-450 family, which is involved in the O-deethylation of 7-EC, is calculated from the turnover number $tn := r_1 r_2/(r_1 + r_2)$ and the monooxygenase activity measured in an air saturated sample. At a substrate concentration of $10^{-4} M$ 7-EC this "active" part amounts to $(15 \pm 2)\%$ independent of the source of the pig liver microsomes. That indicates a constant isoenzyme distribution among different sources and it is in good agreement with the findings of Andersson et al. (1979) obtained at subzero experiments. If we take into account only those forms of cyt. P-450 which are of high affinity towards the 0-deethylation of 7-EC, we calculate a partition of these forms in the transformation that amounts to $(10 \pm 2)\%$ of the total cyt. P-450. However, it must be mentioned that the estimated "active" part does not include that part of cytochrome P-450 which is involved in the autoxidation of the ternary 7-EC-P-450 (Fe^{2+})-O_2 complex, the rate constant of which is unknown.

In *summary* the data presented indicate the ability of the proposed model to describe the relaxation kinetics of product formation. A superposition of two reaction cycles seems not to be necessary to explain the data, when 7-EC is used as a substrate. The model will be helpful in estimating the active part of cyt. P-450 which is involved – in a time average – in various substrate transformations.

References

Andersson KK, Debey B, Balny C (1979) 0-Dealkylation of 7-ethoxycoumarin coupled to single turnover. FEBS Lett 102:117–120

Bansal SK, Love JH, Gurtoo HL (1985) Resolution by high-pressure liquid chromatography and partial characterization of multiple forms of cytochrome P-450 from hepatic microsomes of phenobarbital-treated rats. Eur J Biochem 146:23–33

Ferreira da Silva D, Diehl H (1985) Metabolism of tetra-organolead compounds by rat-liver microsomal monooxygenase. III Enzymatic dealkylation of tetramethyl lead compared with tetraethyl lead. Xenobiotica 15:789–797

Gibson QH, Swoboda BEP, Massey V (1964) Kinetics and mechanism of action of glucose oxidase. J Biol Chem 239: 3927–3934

Guengerich FP (1983) Oxidation-reduction properties of rat liver cytochromes P-450 and NADPH-cytochrome P-450 reductase related to catalysis in reconstituted systems. Biochemistry 22:2811–2820

Guengerich FP, Ghazi AD, Wright ST, Martin MV, Kaminsky LS (1982) Purification and characterization of liver microsomal cytochromes P-450: Electrophoretic, spectral, catalytic, and immunochemical properties and inducibility of eight isoenzymes isolated from rats treated with phenobarbital or β-naphtoflavone. Biochemistry 21:6019–6030

Ihlefeld H, Diehl H (1976) Elementary turnover measurements on the monooxygenase system from liver microsomes: measurement of initial kinetics. FEBS Lett 64: 111–115

Imai Y (1979) Reconstituted 0-dealkylase systems containing various forms of liver microsomal cytochrome P-450. J Biochem 86:1697–1707

Ingelman-Sundberg M, Johansson I (1980) Catalytic properties of purified forms of rabbit liver microsomal cytochrome P-450 in reconstituted phospholipid vesicles. Biochemistry 19:4004–4011

Ingelman-Sundberg M, Haarparanta T, Rydström J (1981) Membrane charge as effector of cytochrome P-450 LM2 catalyzed reactions in reconstituted liposomes. Biochemistry 20:4100–4106

Johnson EF (1979) Multiple forms of cytochrome P-450: Criteria and significance. In: Hodgson E et al. (eds) Reviews in biochemical toxicology 1. Elsevier/North-Holland, Amsterdam, pp 1–26

Jung B, Graf H, Ullrich V (1985) A new monooxygenase product from 7-ethoxycoumarin and its relation to the 0-dealkylation reaction. Biol Chem Hoppe-Seyler 366: 23–31

Komori M, Imai Y, Sato P (1984) Purification and characterization of cytochrome P-450 with high affinity for 7-alkoxycoumarins. J Biochem 95:1379–1388

Lu AYH, Levin W (1972) Partial purification of cytochromes P-450 and P-448 from rat liver microsomes. Biochem Biophys Res Commun 46:1334–1339

Omuta T, Sato R (1964) The carbon monoxide-binding pigment of liver microsomes. I. Evidence for its hemoprotein nature. J Biol Chem 239:2370–2378

Petersen GL (1977) A simplification of the protein assay method of Lowry et al. which is more generally applicable. Anal Biochem 83:346–356

Peterson JA, Ebel RE, O'Keeffe DH, Matsubara T, Estabrook RW (1976) Temperature dependence of cytochrome P-450 reduction. J Biol Chem 251:4010–4016

Provencher SW (1976) An eigenfunction expansion method for the analysis of exponential decay curves. J Chem Phys 64:2772–2777

Ruf HH (1980) Reduction kinetics of microsomal cytochrome P-450. A reexamination. In: Gustafsson JA et al. (eds) Biochemistry, biophysics and regulation of cytochrome P-450. Elsevier/North-Holland Biomedical Press, Amsterdam, pp 355–358

Ruf HH, Eichinger U (1982) Microsomal electron transport. The rate of the electron transfer to oxygenated cytochrome P-450. In: Hietanen E, Laitinen M, Hänninen O (eds) Cytochrome P-450, biochemistry, biophysics and environmental implications. Elsevier/North-Holland Biomedical Press, Amsterdam, pp 597–600

Ryan DE, Thomas PE, Korzeniowski D, Levin W (1979) Separation and characterization of highly purified forms of liver microsomal cytochrome P-450 from rats treated with polychlorinated biphenyls, phenobarbital, and 3-methylcholanthrene. J Biol Chem 254:1365–1374

Ryan DE, Iida S, Wood AW, Thomas PE, Lieber CS, Levin W (1984) Characterization of three highly purified cytochromes P-450 from hepatic microsomes of adult male rats. J Biol Chem 259:1239–1250

Tsuji H, Muta E, Ullrich V (1980) Separation and purification of liver microsomal monooxygenases from induced and untreated pigs. Hoppe-Seyler's Z. Physiol Chem 361: 681–696

Ueno Y, Ishii K, Omata Y, Kamataki T, Kato R (1983) Specificity of hepatic cytochrome P-450 isoenzymes from PCB-treated rats and participation of cytochrome b_5 in the activation of aflatoxin B_1. Carcinogenesis 4:1071–1073

Ullrich V, Weber P (1972) The 0-dealkylation of 7-ethoxycoumarin by liver microsomes. Hoppe Seyler's Z Physiol Chem 353:1171–1177

Ullrich V (1979) Cytochrome P-450 and biological hydroxylation reactions. Top Curr Chem 83:67–104

Werringloer J, Kawano S (1980) The control of the cyclic function of liver microsomal cytochrome P-450: "Counterpoise"-regulation of the electron transfer reactions required for the activation of molecular oxygen. In: Gustafsson JA (eds) Biochemistry, biophysics and regulation of cytochrome P-450. Elsevier/North-Holland Biomedical Press, Amsterdam, pp 359–362

Werringloer J, Kawano S, Kuthan H (1982) Regulation of the cyclic function of liver microsomal cytochrome P-450: on the role of cytochrome b_5. In: Hietanen E, Laitinen M, Hänninen O (eds) Cytochrome P-450, biochemistry, biophysics and environmental implications. Elsevier/North-Holland Biomedical Press, Amsterdam, pp 509–512

White RE, Coon MJ (1980) Oxygen activation by cytochrome P-450. Annu Rev Biochem 49:315–356